De-Noising and Segmentation of Medical Images using Neutrophilic Sets

C. S. Manigandaa[1], V. D. Ambeth Kumar[2*], G. Ragunath[2], R. Venkatesan[3], N. Senthil Kumar[4]

[1] Department of AI&DS, Panimalar Engineering College, Chennai, 600123, India
[2] Department of Computer Engineering, Mizoram University, Aizawl 796004. India
[3]Computer Science and Engineering, Karunya University, Coimbatore 641114, India
[4] Department of Biotechnology, Mizoram University, Aizawl, Mizoram, 796004, India
Emails: csmanigandaa@gmail.com; ambeth@mzu.edu.in; ragunath2004112@gmail.com; rlvenkei_2000@karunya.edu; nskmzu@gmail.com

Abstract

Medical diagnosis and prognosis are challenging tasks due to subjectivity and inherent uncertainty in medical images. Inconsistencies in expert opinions can result in incorrect diagnoses. Neutrosophic theory, a mathematical framework that deals with imprecise or incomplete data, has shown promise in addressing the challenges posed by medical image processing. A neutrosophic theory approach is explored in this paper for de-noising and segmenting medical images. Neutrosophic theory has been utilized to represent the different degrees of truth in each piece of information, resulting in better performance in de-noising and segmentation tasks. Neutosophic theory presents a promising avenue for future investigation in medical image processing as shown in this study.

Keywords: neutrophilic set; medical image; Noise; Segmentation

1. Introduction

Medical images often contain fuzzy and imprecise information, which makes segmentation, feature extraction, and classification challenging. Fuzzy sets have been widely used to process fuzziness and uncertainty in various fields, including image processing and control science. However, the spatial context of pixels is often not considered in these approaches due to noise and artifacts. To address these limitations, the concept of Neutrosophy, introduced by Smarandache , has been increasingly applied in image processing tasks through the use of neutrosophic sets. There are four types of phylogenetic sets in Neutosophic set theory: fuzzy set theory, intervals value fuzzy set theory, and inductive fuzzy set theory, paraconsistent set, paradoxist sets, tautological sets, and dialetheist sets. A>, A> Anti-A>, and A> NonA> refer to concepts, entities, and their opposites and neutrality. A non-neutrosophic logic approach uses the three components of truth, false, and indeterminacy (neither true nor false) to estimate the degrees of inclusion in the truth, the untruth, and the uncertainty. In contrast to fuzzy logic, neutrosophic logic accommodates higher degrees of uncertainty efficiently by introducing an additional domain, I. Fuzzy Sets (FS) and Neutrosophic Sets (NS) differ in that NS allow m to have any value, In contrast, FS requires m to be a 1 (m=t+f).Fig.1 shows the Neutrosophic image domain.

Doi: https://doi.org/10.54216/FPA.110208
Received: December 20, 2022 Accepted: April 26, 2023

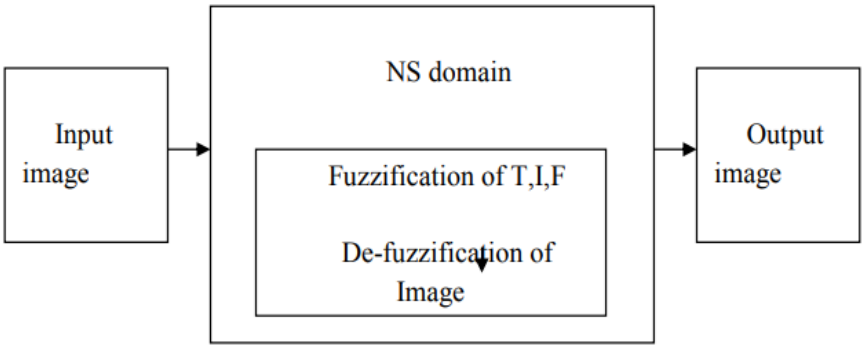

Figure 1. *Neutrosophic Image Domain*

Medical images often contain imprecise and uncertain information; it is difficult for tasks such as feature extraction, segmentation, and classification to be done with accuracy as a result. Various fields have relied upon fuzzy sets for processing uncertainty and fuzziness, they have limitations in their ability to consider spatial context due to noise and artifacts. To address this limitation, the concept of neutrosophy has been introduced, As an image processing method, it is becoming more popular. The concepts of interval fuzzy sets, as well as conventional basic and fuzzy forms, and intuitionistic fuzzy sets include paraconsistent sets, paradoxist sets, tautological sets, and dialetheist sets is expanded upon in neutrosophic set theory.

In a image, Three selections are used to characterise each of the pixels.: truth , indeterminacy , and false . A> stands for the tumor, Neut-A> for the boundaries, and Anti-A> for the backdrop in an image. The A, Neut-A, and Anti-A can be characterised as being represented by the neutrosophic component T, I, and F, respectively. I contains boundary information, while T and F contain information about regions.

Typically, pixels in the image scheme of astronomical photographs are designated by the variables. Methods for segmenting and de-noising data using neutrosophic theory have been suggested in the literature.

An overview of the paper can be found in the following four sections. There are two sections to this chapter: Section 2 describes neutrosophic methods for de-noising and segmenting images, while Section 3 discusses results for several neutrosophic methods. Finally, Section 4 summarizes the conclusion.

2. Image Processing Based on Neutrosophic

2.1. Image Transformation in the Domain of Neutrosophic

The three subsets, which stand for A, Neut, and Anti, respectively, are considered components of neurosophy. Each of the sets of white, undetermined, and non-white pixels are represented by PNI within a neutrosophic pixel, then where TM stands for the white pixels, IM for the undetermined pixels, and FM for the non-white pixels. As a result of computing TM, IM, and FM, the following results are obtained:

$$TM = \frac{\hat{f}_{ij} - \hat{f}_{min}}{\hat{f}_{max}} \quad (1)$$

This equation represents a local mean obtained using window, where i is between 0 and n-1and j is between 0 and m-1, and f is between 0 and max.

$$\hat{f}_{ij} = \frac{1}{w \times w} \sum_{m=i-\frac{w}{2}}^{i+\frac{w}{2}} \sum_{n=j-\frac{w}{2}}^{j+\frac{w}{2}} f_{mn} \quad (2)$$

An image of noise has a size w, the pixels local mean on w has a size f, and an image of noise has a size fmn.

$$IM = \frac{\delta_{ij} - \delta_{min}}{\delta_{max}} \quad (3)$$

$$\delta_{ij} = abs(f_{ij} - \hat{f}_{ij}) \quad (4)$$

Where,

δ_{ij} represents an absolute distinction between the local mean value (f_{ij}) and the magnitude (f_j), max

Doi: https://doi.org/10.54216/FPA.110208
Received: December 20, 2022 Accepted: April 26, 2023

represents the highest relative variance, and min represents the minimal relative difference.
The calculation of the false belonging is

$$FM = 1 - TM \quad (5)$$

Based on Eq. (1), we compute TM by normalizing [0,1] intensity values. In ultrasound pictures, the adjacent mean of the pixel under a kernel can be determined to discriminate between the pixels that belong to textures and speckles. TM is determined by absolute difference, while False subset, FM, is determined by complementing TM.

2.2. Related Research on Image Denoise in the Neutrosophic Domain

To remove Spot disturbance, Gaussian noise, and Rician clamor, a few eliminating methods have been suggested in the writing in light with the neutrosophic set. Images are denoised using a number of NS-based theories and notions. After the picture has been converted from the NS domain, the median filtering process is used to lessen the indecision. The studies were done on real photos with varied amounts of noise in order to improve image denoising.
The wiener filtering process is used to differentiate between true and false subsets to lessen noise and ambiguity. Experiments used Rician noise-affected clinical MR scans and synthetic MRI obtained from the Brainweb database. It was discovered that this wiener filter works well at lowering Rician noise while keeping edges in the neutrosophic domain.
A LEE and KUAN filtering were employed to lessen speckle noise in the neutrosophic domain. The NNRSNR approach, which is based on neutrosophic Gamma statistics, is described in. In neutrosophic space, a further approach is also researched in conjunction with Nakagami takeover values (NTV), which is introduced.

2.3. Related Research on Segmentation of Images in the Neutrosophic Domain

Neutosophic-based approaches for segmenting images issues have lately attracted interest due to their great performance and capacity to handle indeterminacy. A number of NS-based segmentation techniques have been described by a number of authors in the literature. Zhang and co. introduced a solution to the problem of over-segmentation for natural image segmentation in NS that made use of the region merge methodThe area merge algorithm united the two regions starting with the original seeds until the stop requirement is satisfied. fuzzy domain histogram features are used to select the cluster center, and the intensity domain edge value and standard deviation features are used to define the region merge criterion.

The NS approach with image thresholding was developed by Cheng and colleagues to perform indeterminacy-handling segmentation of simulated and real-world images. However, as it is prone to noisy and ignores spatial information, selecting a certain threshold value is an important task. Guo and colleagues first presented the method of fuzzy c-means segmentation for the NS domain. A -mean approach is used to minimise uncertainty and enhance homogeneity after estimating the image's uncertainty using certainty in the NS domains. After that, a fuzzy c-means grouping is used to segment the picture. The uncertainty value is used to update the fuzzy grouping memberships value. According to the findings of the exploratory investigation, the technique performed better on both beautiful and funny images. In this method of NS-based image division, two extra procedures are defined to minimise the rigidity of the picture. Zhang and his fellow researchers developed a ground-breaking strategy for dividing the NS domain. The digital picture is created utilising neutrosophic processing and detection once the image has first been transferred over the NS domain. The watershed approach is used to get the definitive segmentation result. On noisy and uneven images, Neutrosophic Watershed approach performs better.

Enhanced Fuzzy C-Means are added to NS for the objective of IFCM. The affiliation grade and converging criterion definitions are modified as a result. The studies' findings demonstrated that the approach segment the images appropriately and successfully. An innovative method for aggregating uncertain data is neutrosophic C-Means (NCM), It was created utilising the NS architecture and fuzzy c-means methods. Utilising both vagueness denial and proximity disapproval, this method minimises the tendency to cluster challenge, which derives the problem as an objective function. These actions can oversee vulnerability because of uncertain meaning of the groups.

Sengur et al. present yet another approach to automatic segmentation. Which is the NS and wavelet domain combination of texture and color information? This technique segments a natural colour image through K-means clustering. The total amount of K within a cluster is determined via a cluster validation analysis. Experiments demonstrated that it was quite efficient at breaking down the natural images, despite

Doi: https://doi.org/10.54216/FPA.110208
Received: December 20, 2022 Accepted: April 26, 2023

the fact that the texture and colour of each section did not share the same numerical parameters. Shan and co. presented Neutrosophic L-Means (NLM) clustering as a clustering technique for segmenting breast ultrasound images. The method was the most accurate and processed fairly quickly. The method's main drawback is that it fails when subjected to a significant shadowing effect and cannot segment multiple lesions.

A neutrosophic domain colour image segmentation technique has been presented by Karabatak et al. Prior to converting an image to an NS domain, three affiliation sets are defined. The usage of augmentation and mean procedures was utilised to lessen uncertainty. The approach disturbed from set parameters and extensive segmentation. Guo et al. presented an image processing technique built on an NS filter and intensity set. Utilising the grouping sets containing true, false, and inconsistency, the image First is transformed into an NS domain. After that, the noise reducing filter is used and a level for picture segmentation is selected. A new directional -mean operation for edges detection is also presented in the Neutrosophic Edge Detection (NSED) method. The tests have been carried.

The final outcome has been achieved through the use of the DSmT combination rule and decision. The NECM technique is tried on the two information grouping and picture division applications. For ultrasound image breast segmentation, Additionally, the level set methodology and NSS approach are presented. Lastly, an appropriate level set is applied to the NSS image to segment tumours. The results show that the technique can effectively and completely separate the breast tissue from the tissue surrounding it in ultrasound pictures.

3. Outcomes of the research and discussions

3.1. Enhancing outcomes for synthetic images

This section demonstrates an unbiased comparison of neutrosophic domains speckled reduction techniques. SNR and Corner Preservation Index are two quantitative metrics that have been used to evaluate the aforementioned techniques. A speckle simulation procedure is used for quantitative evaluation of despeckling methods. This procedure corrupts images by creating speckle noise. A synthetic image with noise levels ranging from 0.4 to 0.10 is presented in Table 1. By achieving higher SNR. Statistically, neutrosophic domain approaches dominate space-domain approaches. Due to their superior efficiency, NKUAN's SNR ratings are greater than KUAN's. A higher SNR has also been achieved by NLEE compared to LEE.

Table 1: SNR value of noisy image's

SN ratio					
Level	Noisy Image	KUA	NKUA	LE	NLE
0.4	21.1	22.00	23.22	23.78	23.87
0.5	19.4	20.45	21.4	21.52	22.33
0.6	17.09	18.71	19.37	20.5	21.52
0.7	16.8	17.01	18.84	19.1	20.46
0.8	15.2	15.28	16.33	17.6	18.92
0.9	13.9	14.60	15.94	16.4	17.51
0.10	3.3	5.20	6.0	7.7	8.53

The figure below shows how neutrosophic domain methods preserve edges better than spatial domain methods for various speckle reduction techniques. Fig. shows a graphic representation of the situation. As observed in 2, NLEE is more capable of preserving edges in neutrosophic domains than LEE. It has also been found that the NLEE method does a better job of preserving edges than NKUAN. The outcomes were contrasted with those attained by spatial-domain speckled elimination filtering like the LEE and KAUN. Figure 3 depicts a synthetic picture with speckles. Fig. Figure 3(a) shows the original image, whereas Figure 3 shows the modified version. Speckle noise has been simulated in Figure 3(b) at a noise level of 0.5. The despeckling outcomes of the LEE and KUAN filters are depicted in Figures 3(c) and (d), respectively. Figure 3(e) and 3(f) illustrate the results of the recommended methods, the KUAN NKUAN filter as well as the NLEE filter.

Doi: https://doi.org/10.54216/FPA.110208

Received: December 20, 2022 Accepted: April 26, 2023

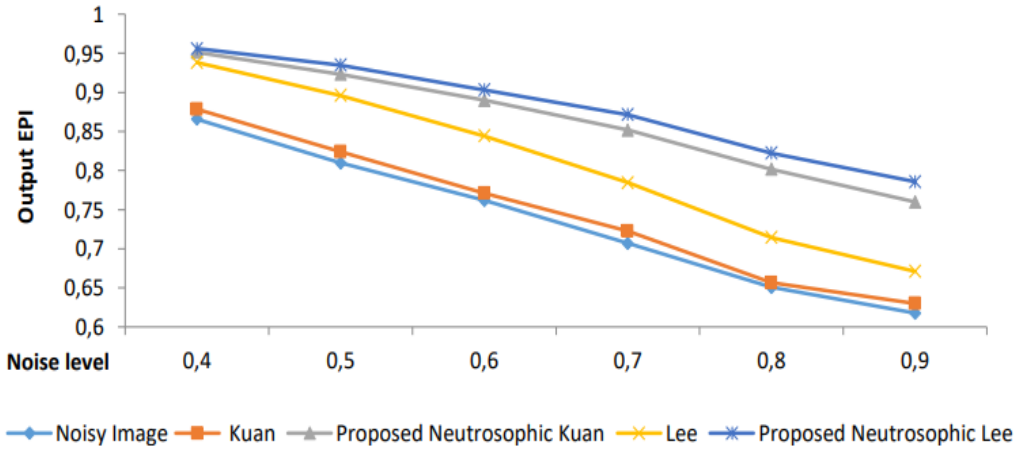

Figure 2: Comparing the effectiveness of various techniques for speckle simulation on synthetic images using EPI.

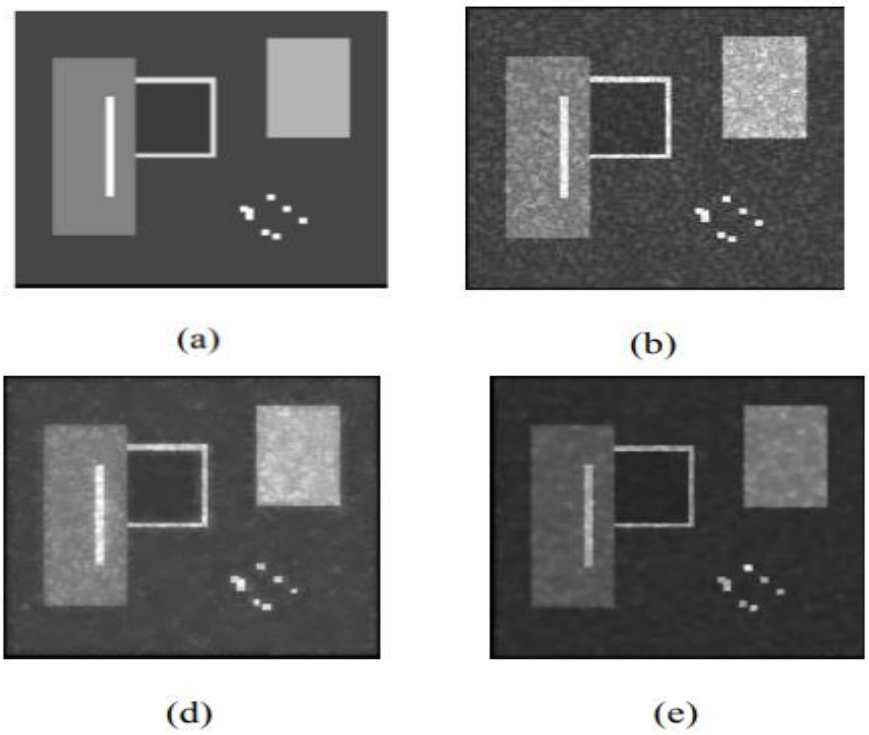

Figure 3: (a) norma; image (b) Speckle image (d) KUA (e) NKUA

Table 2 contrasts SNR determines for streaks decreased techniques as NTV, NNTV, NNRSNR , at various noise levels ranging from = 0.4 to 0.10. The quantitative findings show that the neutrosophic subdomain NNRSNR strategy outperforms the NRSNR approach by obtaining better SNR values. Similar to how neutrosophic domain NNTV performed better than NTV and other approaches due to its greater SNR value. By reaching maximal SNR values, Table 2 makes clear that despite elevated levels of noise, both neutrosophic domain techniques performed better than their alternatives.

Doi: https://doi.org/10.54216/FPA.110208
Received: December 20, 2022 Accepted: April 26, 2023

Table 2: SNR caluculated in dB, was compared among different methods at various levels of noise (σ ranging from 0.4 to 0.10).

Range	Image	NRSN	NNRSN	NT	NNT
0.4	21.10	22.7	24.27	25.37	26.84
0.5	19.0	22.10	23.06	23.74	24.36
0.6	17.93	22.43	23.77	24.26	25.81
0.7	16.35	21.67	21.91	22.74	23.0
0.8	15.22	18.76	19.63	20.94	21.77
0.9	13.97	17.27	18.32	20.17	20.86
0.10	3.62	6.80	8.75	9.63	10.31
Average	15.53	18.88	19.99	20.91	21.88

Similar observations can be drawn from Fig. In this speckle-simulated phantom picture, perceptual comparison across NRSNR, NTV, NNRSNR, with NNTV is apparent. Figure 4(a) shows the unaltered version of the photograph, whereas Figure 4 shows the edited version. Figure 4 displays a photo of speckles.(b). While Figure 4 illustrates how the NRSNR obscured image details like edges.(c). Figure 4 shows how well the NNRSNR technique, which is based on the neutrosophic domain, suppresses speckles.(d). However, artificial suppression and blurring near the edges damage some pixels. Figures 4(e) and 4(f) show a similar type of observation, namely that the neutrosophic domain NNTV approach produces better visual results.

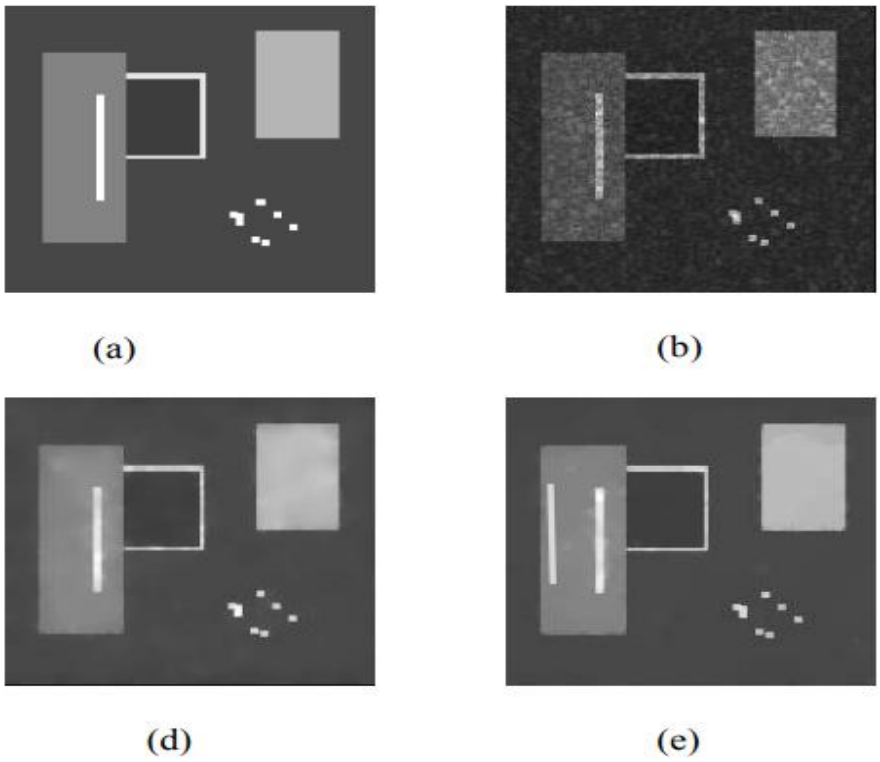

Figure 4: (a) Normal image (b) Speckle. Image processed by (d) NNRSN (e) NT

3.2 De-noising techniques results on real images

The outcomes of the KAN, LEE, and NLEE approaches on images are displayed in Figure 5. In Figure 5, the original picture is displayed. (a). By eliminating speckle noise, NKUAN and NLEE techniques performed better than the KUAN and LEE techniques in the spatially domain, as shown in Fig. 5.

Doi: https://doi.org/10.54216/FPA.110208
Received: December 20, 2022 Accepted: April 26, 2023

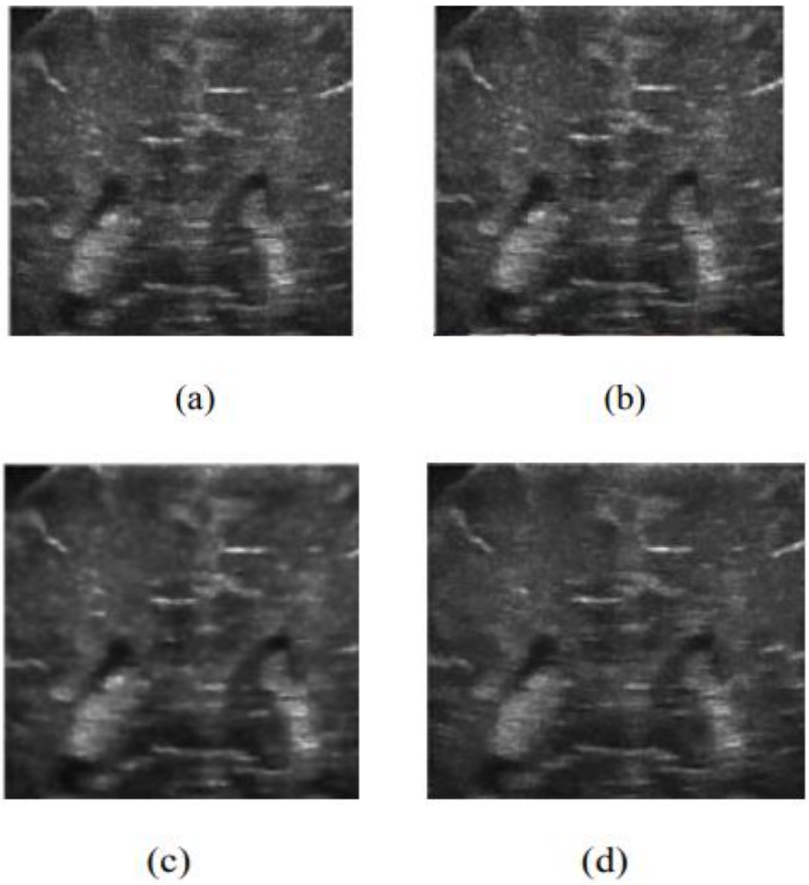

Figure 5: comparison on (a) image (b) KUA technique (c) NKUA technique (d) LE technique

Figure 6 displays the outcomes obtained using the NRSN, NT, NNT, and NNRSN approaches on ultrasound. Fig. 6 provides the ultrasound (a). While speckle reduction, as shown in Fig. 6, was being done, the NRSNR oversmoothed and smudged the pictures (b). Important image features and information were lost as a result. Better results were obtained using the NNRSNR technique, but artefacts may be seen in Fig. 6(c). After being processed by neutrosophic subdomain speckle reduction techniques, little structures that are hidden by noise from speckles become visible. The NNTV may maintain anatomical structures, resolvable features, and boundaries while removing speckle patterns. All of these findings show how effective neutrosophic domain techniques are in dealing with uncertainty. The line profiles of these visual results, which follow the line in the primary image, are also examined. By reducing noise from speckles and keeping the margins and borders in a thyroid imaging picture, as can be seen by taking a closer look at Figs. 7(d) and 7(f) in this regard. The techniques in the neutrosophic domain can keep the image's corners, limits, and crisp features as demonstrated in Fig.7.

Doi: https://doi.org/10.54216/FPA.110208

Received: December 20, 2022 Accepted: April 26, 2023

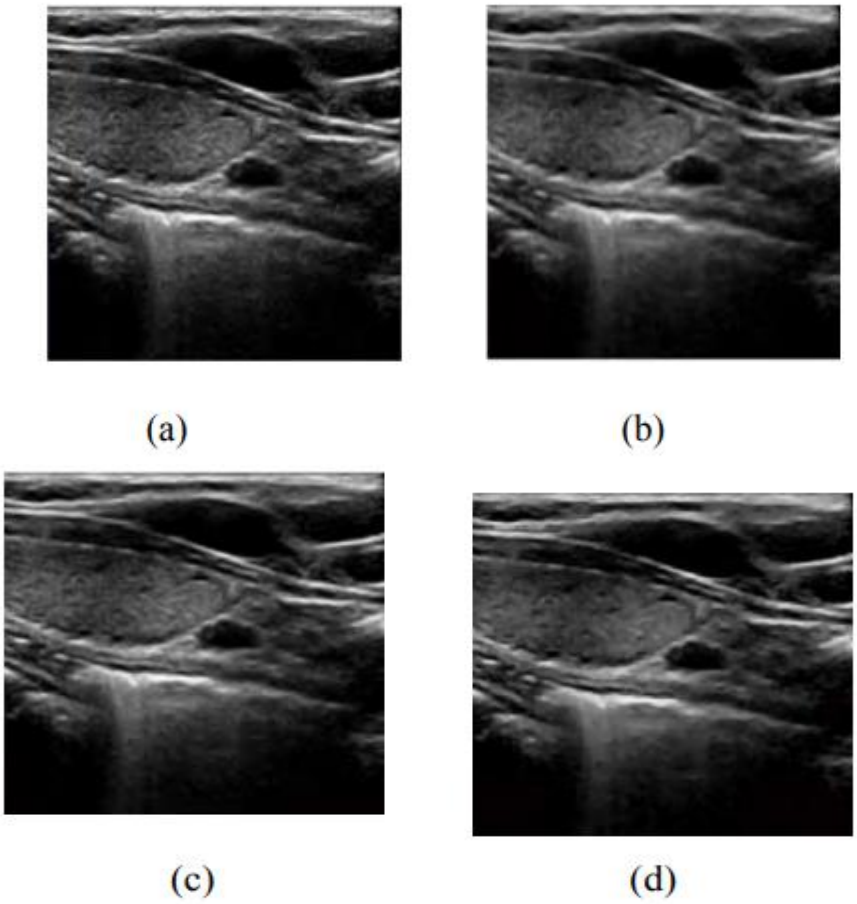

Figure 6: Results on the thyro-ultrasound (a) image. image by (b) NRSN technique (c) NNRSN technique (d) NT technique.

It may maintain anatomical structures, resolvable features, and boundaries while removing speckle patterns. All of these findings show how effective neutrosophic domain techniques are in dealing with uncertainty. The line profiles of these visual results, which follow the line in the primary image, are also examined. By reducing noise from speckles and keeping the borders and corners in a thyroid ultrasound image, as can be seen by taking a closer look at Figs. 7(d) and 7(f) in this regard. The techniques in the neutrosophic domain can keep the image's corners, limits, and crisp features as demonstrated in Fig.8.

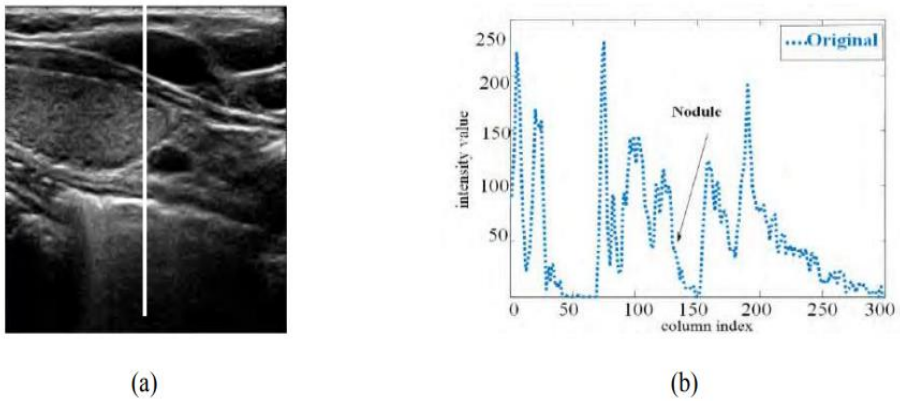

Figure 7: Line for thyroid ultrasound (a) Original image. (b) Line of original image.

Doi: https://doi.org/10.54216/FPA.110208
Received: December 20, 2022 Accepted: April 26, 2023

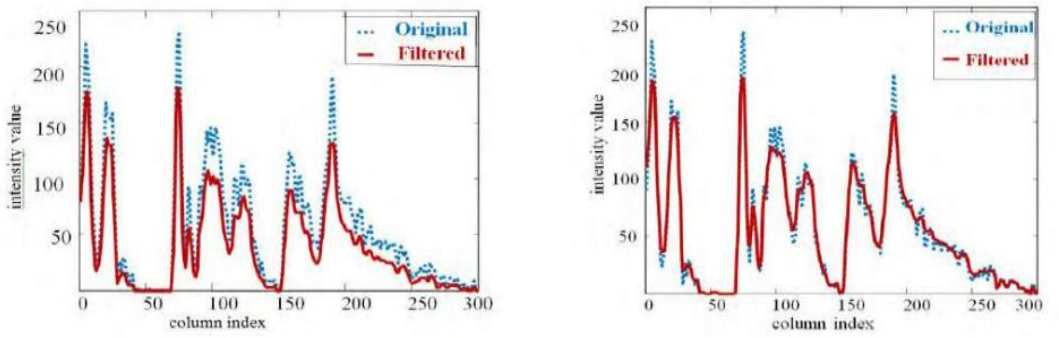

(c) (d)

Figure 7 (Continued): Line for thyroid ultrasound (c) NRSN technique (d) NNRSN technique

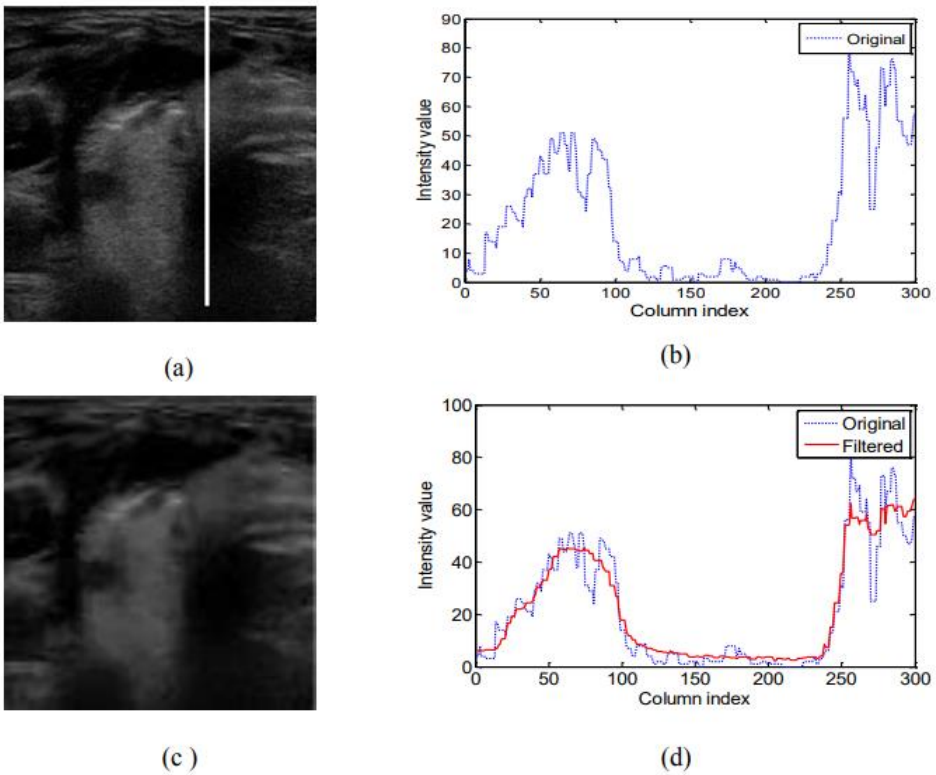

(a) (b)

(c) (d)

Figure 8: De-noising the thyro-image (a) image (b) Line of image (c) NNRSN (d) NNRSN.

3.3. The outcomes of segmentation based on real image

In addition, genuine ultrasound images are used to compare the efficiency of neutrosophic sphere segmentation methods.Table 3 displays the values for each quality criterion. Results show that, by reaching high values across a variety of performance measures, SNDRLS beats any other neutrosophic field techniques. The retrieved area and the physical truth are more comparable thanks to the additional area-based metrics specified by the SNDRLS method. Additionally, as shown in Table 3, the SNLM outperforms other approaches in terms of FP and HD values. According to the findings, the SNDRLS approach covers a larger region.

Doi: https://doi.org/10.54216/FPA.110208
Received: December 20, 2022 Accepted: April 26, 2023

Table 3: Effectiveness of various methods of segmentation

Methods	TPM (%)	DCM(%)	FPM(%)	HDM
NC	83.5 ± 6.1	78.57 ± 18.3	10.73 ± 10.9	22.1 ± 19.5
NL	83.0 ± 5.7	84.00 ± 3.9	13.31 ± 13.7	4.7 ± 4.0.3
SNL	94.45 ± 2.0	92.7 ± 6.6	4.77 ± 4.4	3.27 ± 0.4
SNDRL	97.92 ± 3.20	91.88 ± 2.57	7.0 ± 4.11	0.51 ± 0.2

Subjective outcomes are added to the proposed method's quantitative results. The proposed SNDRLS approach is compared to all of the other methods in Figure 9. The original ultrasound of the thyroid image is shown in Figure 9(a), and the ground truth image is shown in Figure 9(b). As depicted in Fig. 9, It should be noticed the way the NW contoured split crosses the weak boundaries (c).

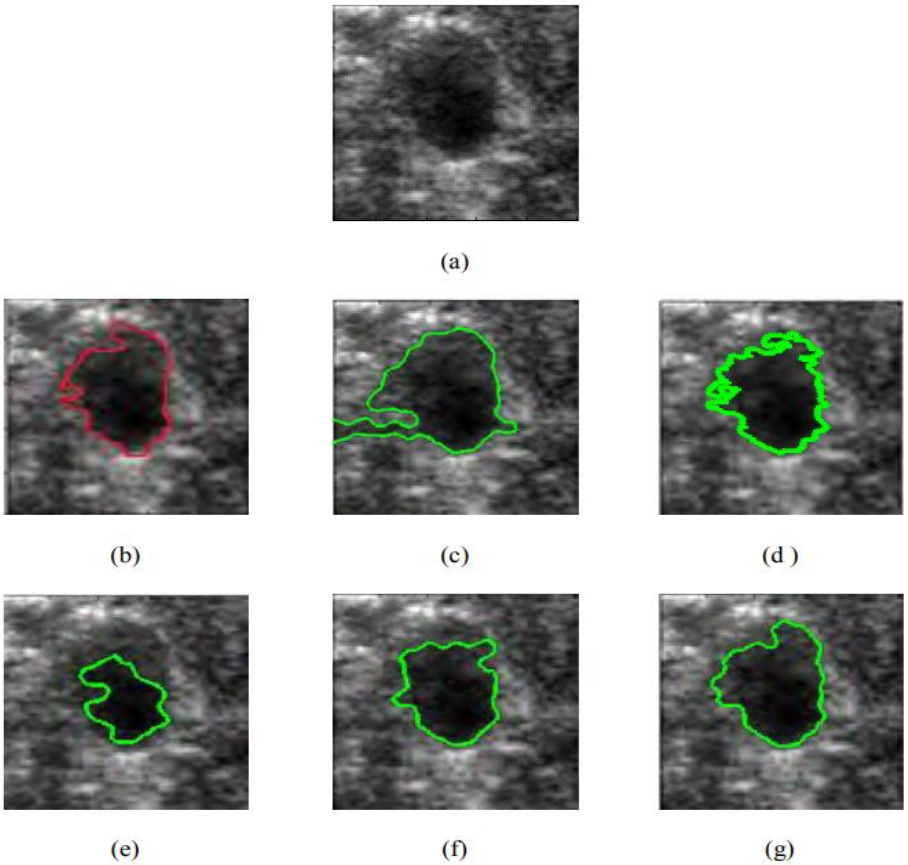

Figure 9: (a) Ultrasound image (img23) (b) Ground Truth. Segmentation results by (c) Neutrosophic Watershed (NW) [33] (d) NCM [35] (e) NLM [37] (f) SNLM [44] (g) SNDRLS [44].

NCM is affected, as depicted in Fig. 9, since it is easily caught within incorrect localized extremes because of similar strengths.(d). The NLM technique fails to properly fragment nodule, as shown in Fig. 9(e). The result of SNL is also shown in Fig. 9(f), which demonstrates that the outermost portion of the segmented nodules does not lie close to the line specified by an expert. As can be seen in Fig. 9, the SNDRLS results are remarkably similar to the manual segmentation.(g). The SNDRLS can deal with the fuzziness,

Doi: https://doi.org/10.54216/FPA.110208
Received: December 20, 2022 Accepted: April 26, 2023

uncertainty, and indeterminacy of pixels. It has been shown from the visual results that the SNDRLS approach is efficient and precise in nodule segmentation utilising ultrasound pictures. The original ultrasound figure is depicted in Figure 10(a) and (b). Due to weak borders and low contrast, it is clear from Fig. 10(c) that the nodular is not correctly segmented out. As demonstrated in Fig. 10, the picture segmentation by NLM has the capacity to differentiate nodule regions from non-nodule regions.10(d).

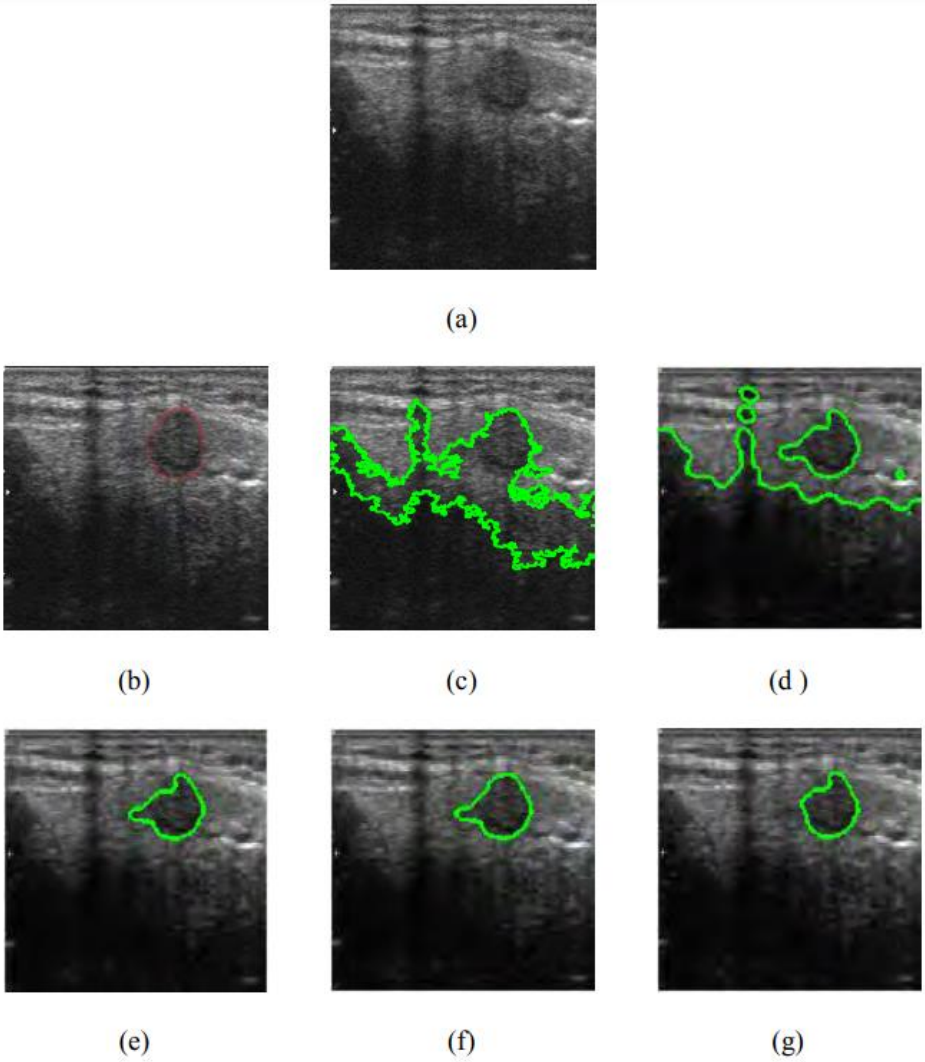

Figure 10: Ultrasound image (img318) (a) Original image (b) Ground Truth. Segmentation results by (c) NW [33] (d) NLM [37] (e) SNLM [44] (f) NCM [35] (g) SNDRLS [44].

The ability of the NCM and SNLM to separate a nodules from the neutrosophic domain is demonstrated in Figures 10(e) and 10(f), despite the fact that the resulting border is not very near the solid true boundaries.(f).

SNDRLS achieves superior nodular the process of segmentation as seen in Fig. 10, because the obtained delineations are highly smooth and perfectly fitted to the nodule's borders.(g).

Additionally, SNDRLS can effectively handle intensity in-homogeneity, preventing leakage across weak edges leading to precise extraction of nodule borders.

4. Conclusion

With the help of neutrosophic logic, an image with uncertain information can be described in a powerful way. Denoising and segmentation of medical images using neutrosophic theory are discussed in this paper.

Doi: https://doi.org/10.54216/FPA.110208

Received: December 20, 2022 Accepted: April 26, 2023

By virtue of its indeterminacy handling capability, neutrosophic set is able to handle a greater number of uncertainties than fuzzy/non fuzzy set theory. Despite low contrasted images and vague borders/regions, the neurosophic set provides better results. By analysing the work presented previously, we observe that neutrosophic methods are appropriate for a number of applications, including pattern detection and image processing. Additionally, it aids in resolving issues brought on by human error when designing the membership function.

Funding: "This research received no external funding"

Conflicts of Interest: "The authors declare no conflict of interest."

References

[1] Mondal K, Dutta P, Bhattacharyya S. Fuzzy logic based gray image extraction and segmentation. International Journal of Scientific & Engineering Research. 2012;3(4):1-14.
[2] Yang Y, Huang S. Image segmentation by fuzzy C-means clustering algorithm with a novel penalty term. Computing and Informatics. 2012;26(1):17-31.
[3] Koundal D, Gupta S, Singh S. Applications of neutrosophic and intuitionistic fuzzy set on Image processing. National Conference on Green Technologies: Smart and Efficient Management (GTSEM-2012). 2012.
[4] Smarandache F. A Unifying Field in Logics: Neutrosophic Logic. Neutrosophy, Neutrosophic Set, Neutrosophic Probability: Neutrosophic Logic. Neutrosophy, Neutrosophic Set, Neutrosophic Probability. Infinite Study; 2005.
[5] Zhang M, Zhang L, Cheng HD. Segmentation of ultrasound breast images based on a neutrosophic method. Optical Engineering. 2010;49(11): 117001-117001.
[6] Atanassov KT. Intuitionistic fuzzy sets. Fuzzy sets and Systems. 1986;20(1):87-96.
[7] Zhang L, Zhang Y. A novel region merge algorithm based on neutrosophic logic. International Journal of Digital Content Technology and its Applications. 2011;5(7):381-7.
[8] Smarandache F. A Geometric Interpretation of the Neutrosophic Set-A Generalization of the Intuitionistic Fuzzy Set. arXiv preprint math/0404520. 2004.
[9] Zhang M. Novel approaches to image segmentation based on neutrosophic logic. (Doctoral dissertation, Utah State University). 2010.
[10] Ju W. Novel Application of Neutrosophic Logic in Classifiers Evaluated under Region-Based Image Categorization System (Doctoral dissertation, Utah State University). 2011.
[11] Smarandache F. Neutrosophic Logic-Generalization of the Intuitionistic Fuzzy Logic. arXiv preprint math/0303009. 2003.
[12] Wang H, Smarandache F, Sunderraman R, Zhang YQ. Interval Neutrosophic Sets and Logic: Theory and Applications in Computing: Theory and Applications in Computing. Infinite Study. 2005(5).
[13] Cheng HD, Shan J, Ju W, Guo Y, Zhang L. Automated breast cancer detection and classification using ultrasound images: A survey. Pattern Recognition. 2010;43(1):299-317.
[14] Eisa M. A New Approach for Enhancing Image Retrieval using Neutrosophic Sets. International Journal of Computer Applications. 2014;95(8):12-20.
[15] Shan J. A fully automatic segmentation method for breast ultrasound images. (Doctoral dissertation, Utah State University). 2011.
[16] Guo Y, Cheng HD, Zhang Y. A new neutrosophic approach to image denoising. New Mathematics and Natural Computation. 2009 Nov;5(3):653-62.
[17] Guo Y, Şengür A. A novel image segmentation algorithm based on neutrosophic filtering and level set. Neutrosophic Sets and Systems. 2013;1:46-49.
[18] Mohan J, Chandra AT, Krishnaveni V, Guo Y. Evaluation of Neutrosophic Set Approach Filtering Technique For Image Denoising. The International Journal of Multimedia & Its Applications (IJMA). 2012;4(4):73-81.
[19] Mohan J, Chandra AT, Krishnaveni V, Guo Y. Image Denoising Based on Neutrosophic Wiener Filtering. In Advances in Computing and Information Technology. Springer Berlin Heidelberg. 2013;861-869.
[20] Mohan J, Krishnaveni V, Guo Y. Performance analysis of neutrosophic set approach of median filtering for MRI denoising. Int. J Elec. & Commn. Engg & Tech. 2012;3:148-163.
[21] Mohan J, Krishnaveni V, Guo Y. MRI denoising using nonlocal neutrosophic set approach of Wiener filtering. Biomedical Signal Processing and Control. 2013;8(6):779-791.

Doi: https://doi.org/10.54216/FPA.110208

Received: December 20, 2022 Accepted: April 26, 2023

[22] Mohan J, Krishnaveni V, Guo Y. A new neutrosophic approach of wiener Filtering for MRI denoising. Measurement Science Review. 2013;13(4):177-186.
[23] Qi X, Liu B, Xu J. A Neutrosophic Filter for High-Density Salt and Pepper Noise Based on Pixel-Wise Adaptive Smoothing Parameter. Journal of Visual Communication and Image Representation. 2016;36:1-10.
[24] Guo Y, Cheng HD, Zhao W, Zhang Y. A novel image segmentation algorithm based on fuzzy c-means algorithm and neutrosophic set. Proceeding of the 11th Joint Conference on Information Sciences, Atlantis Press. 2008.
[25] Lee JS. Digital image enhancement and noise filtering by use of local statistics. Pattern Analysis and Machine Intelligence, IEEE Transactions on. 1980;(2):165-168.
[26] Kuan DT, Sawchuk AA, Strand TC, Chavel P. Adaptive restoration of images with speckle. In 26th Annual Technical Symposium of International Society for Optics and Photonics. 1983: 28-38.
[27] Koundal D, Gupta S, Singh S. Speckle reduction method for thyroid ultrasound images in neutrosophic domain. IET Image Processing. 2016;10(2):167-75.
[28] Koundal D, Gupta S, Singh S. Speckle reduction filter in neutrosophic domain. In Int. Conf. of Biomedical Engineering and Assisted Technologies. 2012:786-790.
[29] Koundal D, Gupta S, Singh S. Nakagami-based total variation method for speckle reduction in thyroid ultrasound images. Proceedings of the Institution of Mechanical Engineers, Part H: Journal of Engineering in Medicine. 2016; 230(2):97-110.
[30] Koundal D. Automated system for delineation of thyroid nodules in ultrasound images. 2016 (Doctoral dissertation, Panjab University, Chandigarh, India).
[31] Cheng HD, Guo Y. A new neutrosophic approach to image thresholding. New Mathematics and Natural Computation. 2008;4(03):291-308.
[32] Guo Y, Cheng HD. New neutrosophic approach to image segmentation. Pattern Recognition. 2009;42(5):587-595.
[33] Zhang M, Zhang L, Cheng HD. A neutrosophic approach to image segmentation based on watershed method. Signal Processing. 2010;90(5):1510-1517.
[34] Guo Y, Sengur A. A novel color image segmentation approach based on neutrosophic set and modified fuzzy c-means. Circuits, Systems, and Signal Processing. 2013;32(4):1699-1723.
[35] Guo Y, Sengur A. NCM: Neutrosophic c-means clustering algorithm. Pattern Recognition. 2015;48(8):2710- 2724.
[36] Sengur A, Guo Y. Color texture image segmentation based on neutrosophic set and wavelet transformation. Computer Vision and Image Understanding. 2011;115(8):1134-1144.
[37] Shan J, Cheng HD, Wang Y. A novel segmentation method for breast ultrasound images based on neutrosophic l-means clustering. Medical physics. 2012;39(9):5669-5682.

Doi: https://doi.org/10.54216/FPA.110208

Received: December 20, 2022 Accepted: April 26, 2023